[Frontiers in Bioscience E4, 1571-1581, January 1, 2012]

A modified histoimmunochemistry-assisted method for *in situ* RPE evaluation

Jingfa Zhang[1,4], Guoxu Xu[2], Limei Zhang[4], Limin Gu[4], Hua Xu[4], Lixia Lu[1,4], Juan Wang[1,4], Furong Gao[1,4], Jing-Ying Xu[1,4], Fang Wang[1], Weiye Li[1,3,4], Guo-Tong Xu[1,4]

[1]Department of Ophthalmology, Shanghai Tenth People's Hospital, and Tongji Eye Institute, Tongji University School of Medicine, Shanghai, China, [2]Department of Ophthalmology, Second Affiliated Hospital of Soochow University, Suzhou, China, [3]Department of Ophthalmology, Drexel University College of Medicine, Philadelphia, PA, USA, [4]Stem Cell Research Center and Department of Regenerative Medicine, Tongji University School of Medicine, Shanghai, China

TABLE OF CONTENTS

1. ABSTRACT

We have developed a method for morphological evaluation of retinal pigment epithelium (RPE) with minimal perturbation of RPE-Bruch's membrane-choriocapillaris complex (RBCC). To prepare RBCC, the anterior segments of the eye were removed. The remaining eye cup was radially cut into 4 to 6 pieces from periphery to the optic nerve head. Each piece was carefully dissected into 3 parts: sclera, RBCC and neurosensory retina. RBCC flatmount with RPE monolayer facing up was formed by several relaxing radial cuts. After immuno-staining with tissue specific markers, the RBCC could be distinguished as the superficial RPE monolayer and the underneath choriocapillaris layers by fluorescence microscopy. The density, distribution, and morphology of RPE cells varied among species. This method may have brought several advantages for RPE screening over other means, because of its straight forward approach, minimal manipulation of samples, plus there is no requirement for bleaching, which result in high efficiency for result readout. For a complete morphological study of RPE *in situ*, this method may be combined with other methods, such as cryosections, scanning electron microscopy, etc.

2. INTRODUCTION

Retinal pigment epithelium (RPE), a monolayer of highly polarized pigmented cells located between the neurosensory retina and the Bruch's membrane-choriocapillaris, plays a critical role in the maintenance of visual function (1). The main functions of the RPE include: transport of nutrients, ions, and water; absorption of light and protection against photooxidation; reisomerization of all-trans-retinal into 11-cis-retinal; phagocytosis of shed photoreceptor membranes; secretion of various essential factors for the structural integrity of the retina; stabilization of ion composition in the subretinal space, which is crucial for the maintenance of photoreceptor excitability; and contribution to the immune privileged status of the eye as part of the blood-retinal barrier (BRB) and by the secretion of immunosuppressive factors inside the eye, etc (2-4). Thus, RPE is essential for neuroretina survival and, consequently, for visual function.

Alterations in the RPE monolayer play a role in physiological aging and of pathological processes. Dysfunction of the RPE may lead to the pathogenesis of a wide variety of sight-threatening diseases, including

hereditary disorders such as retinitis pigmentosa (5-8), Stargardt's disease (9), and acquired age-related macular degeneration (AMD) (10, 11). RPE cells are therefore of great interest to researchers for studying its pathophysiological changes in retinal disorders.

Several models are used to mimic the pathophysiological changes of RPE cells. Cell culture is a well-established technique to study RPE cells (12-14), but the *in vitro* results do not fully reflect the real changes of RPE cells in disease conditions. Animal models are also employed to mimic the pathological changes of RPE cells in human, e.g., sodium iodate induced RPE cell damage in mice and rats (15-17), and the Royal College of Surgeons (RCS) rat (18, 19), etc. In these animal models, the RPE morphology was widely studied by cross sections. Anatomical abnormalities, such as disruptions in the RPE monolayer and decrease in the numbers of RPE cells, were evidenced in cross-sections of sodium iodate injected mice (16). But the cross-sections (cryosection and paraffin section) cannot totally demonstrate the morphological changes of RPE cells, at least not the entire RPE layer. RPE cells can also be observed by scanning and transmission electron microscope with more specific changes on the ultrastructural levels (20, 21). However, the processes are complicated, and the *en bloc* examination to get an overview of RPE changes was limited by the electron microscopy.

Because of the limitations of current techniques, we have developed a method for a comprehensive morphological evaluation of RPE cells, with minimal perturbation of RPE-Bruch's membrane-choriocapillaris complex (RBCC). This method may have several advantages to screen the changes of RPE than other means, because of its straight forward approach, minimal manipulation of samples, *en bloc* examination, no requirement for bleaching, and high efficiency for result readout. However, for a completed morphological study of RPE, this method may still be combined with other methods, such as cryosections, scanning or transmission electron microscopy, etc.

3. MATERIALS AND METHODS

3.1 Reagents

All biochemical reagents were of analytical grade and purchased from commercial suppliers. RPE65 (8B11) antibody (sc-53489) was purchased from Santa Cruz Biotechnology; Isolectin GS-IB4 (121411) was purchased from Invitrogen; Fluorescein (FITC)-conjugated AffiniPure Goat anti-mouse IgG (H+L) (115-095-003) and CY3-conjugated AffiniPure Goat anti-mouse IgG (H+L) (115-165-003) were purchased from Jackson ImmunoResearch. Dako Fluorescent Mounting Medium (S3023) was from Dako North America, Inc.

3.2 Experimental animals and sodium iodate (SI)-induced RPE degeneration rat model

The Sprague-Dawley (SD) rats, New Zealand white rabbits and mice were from Slaccas (SIBS, Shanghai, China). The animals were treated in accordance with the ARVO Statement for the Use of Animals in Ophthalmic and Vision Research. The rats, rabbits and mice were killed with an overdose of pentobarbital sodium. Both eyes were enucleated, fixed in 1x PBS buffered 4% paraformaldehyde solution, and stored at 4 ^{o}C until use. For better fixation, a window cut was made in sclera. The eyes of the domestic pig were from the local Slaughterhouse, and the eyes of monkey were a gift of the Lingkang Sainuo Biotech. Co. Ltd. (Nanning Guangxi, China).

To establish the SI-induced RPE degeneration model, SD rats (body weight, 200 g ±) were intravenously injected with SI solution (dissolved in normal saline, 50 mg/kg BW) (Sigma, St. Louis, MO, USA). The rats were killed and both eyes were enucleated at the following time points: 6, 12 hours, and 1, 3, 7, 14 and 28 days after SI injection. Normal rats injected with saline served as controls. The RBCCs from two individual eyes of different rats per time point were studied.

3.3 RBCC isolation and immunohistochemistry study

Under a dissection microscope, the muscles and connective tissues of rabbit were removed from the eye ball; the anterior segments of the eye including cornea, iris and lens were carefully removed. Then, the eye cup was radially cut into 4 to 6 pieces from periphery to the optic nerve head. Each piece was carefully dissected into 3 parts: sclera, RBCC and neurosensory retina (Figure 1).

For immunostaining, RBCC was washed thoroughly in 1x PBS and incubated with PBS containing 0.25% Triton X-100 (0694-1L, Amresco) for 10 minutes to improve the penetration of the antibody. After immersion for 30 minutes in PBS containing 0.1% Tween 20 (0777-1L, Amresco) and 1% bovine serum albumin (A2153, Sigma-Aldrich), RBCC was incubated with the primary antibody (mouse anti-RPE65 antibody, 1:100, Santa Cruz, sc-53489) with or without Isolectin GS-IB4 (1:100, Invitrogen, 121411) in blocking buffer overnight at 4 ^{o}C. RBCC was then rinsed in PBS, incubated with the appropriate secondary antibody (1:100, anti-mouse FITC or anti-mouse CY3) for 1 hour at room temperature in dark. After washing thoroughly in PBS for 15 minutes, the RBCC was then incubated with 1 μg/mL DAPI (4', 6'-Diamidino-2-phenylindole, 32670, Sigma-Aldrich) for 1 minute, then rinsed again thoroughly in PBS, and then mounted with mounting medium (DakoCytomation Fluorescent Mounting Medium, S3023, Dako North America, Inc.) with RPE monolayer facing up. Normally, RBCC was coiling after peeling from sclera, the inside of RBCC is RPE monolayer. When flattening RBCC, make sure that RPE monolayer is upward, and flatten it by 2-3 relaxing cuts. The RBCC was then observed by fluorescence microscope (200x and 400x, Nikon, Japan).

4. RESULTS

4.1. The procedure for RBCC isolation and observation

The detailed procedure for isolation of RBCC was shown in Figure 1. Under the dissection microscope, the anterior segments of the eye (cornea and iris) and lens were gently removed. The remaining eye cup was radially cut into 4 to 6 pieces from periphery to the optic nerve

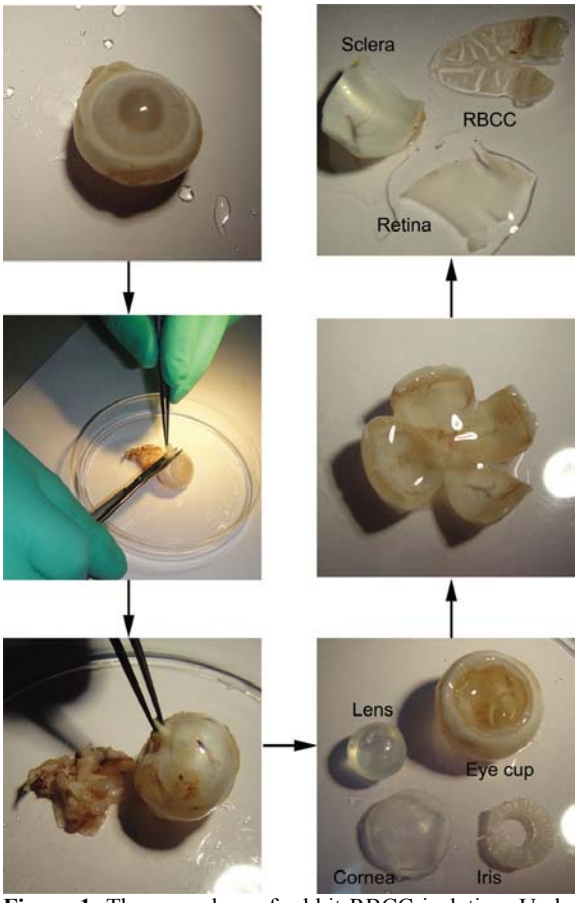

Figure 1. The procedure of rabbit RBCC isolation. Under dissection microscope, the muscles and connective tissues of rabbit were removed from the eye ball; the anterior segments of the eye including cornea, iris and lens were carefully removed. Then, the eye cup was radially cut into 4 to 6 pieces from periphery to the optic nerve head. Each piece was carefully dissected into 3 parts: sclera, RBCC and neurosensory retina. The arrows indicate the flow of this procedure.

head. Each piece was carefully dissected into 3 parts: sclera, RBCC and neurosensory retina.

Before examination under microscope, RBCC flatmount was flattened by several relaxing cuts, depending on the size of the RBCC, with RPE monolayer facing up. When stained with DAPI, the RPE cells, with big, round nuclei, can be clearly identified under fluorescence microscope (Figure 2); the density, size and distribution of RPE nuclei varied among species. After staining with the specific markers for both RPE cells (RPE 65 antibody) and choricapillaris endothelial cells (CCEs, Isolectin), the RBCC was roughly divided into 2 layers: the superficial RPE monolayer and the underneath choriocapillaris layers (Figure 3).

The RBCC was observed under scanning electronic microscope (SEM). The microvilli (Figure 4A), the characteristic cell bodies (Figure 4B) and the artificial detachment of RPE cells from the Bruch's membrane (Figure 4C) was observed under SEM. By using SEM when scanning at the microvilli level, multiple holes were observed (Figure 4A). The detachment of RPE cells was observed under fluorescence microscope, leaving the Bruch's membrane completely bare (Figure 4D).

4.2. The morphology and distribution of the microvilli

The morphology and size of the microvilli of the RPE cells vary among the species. They look thinner in the eyes of mice, rat and rabbit; and much larger in the domestic pig and monkey (Figure 5). In rabbit, pig and monkey eyes, when the superior surface of the microvilli was in focus, the microvilli of RPE cells present as the several holes, as observed in rat under SEM (Figure 4A), where the outer segments of photoreceptors and the RPE cells are intertwining (Figure 5). When further focusing downward, beyond the level of microvilli, the RPE cell bodies were identified (Figure 6).

The distributions of the microvilli also vary among species. In rabbit, the microvilli are dense in peripheral RPE; less in central RPE, and nearly no microvilli detected in Mid-RPE (Figure 7); in a monkey eye, the density of the microvilli gradually decreases from the peripheral to the central RPE (Figure 7). The dense microvilli in peripheral RPE and scarce in central RPE indicate the different intertwining pattern between RPE cells and photoreceptors in periphery and in central retina, suggesting a trend showing more microvilli interacting with a single photoreceptor in periphery than in center.

4.3. Pigmented RPE cells can be detected without bleaching

To detect the optimal conditions for the study of pigmented RPE cells, the RBCCs of pigmented domestic pig eye were comparatively studied with or without bleaching with hydrogen peroxide before immunostaining with RPE 65. In the preparation of the RBCC without bleaching, RPE cells were clearly observed under the fluorescence microscope (Figure 8); however, after bleaching for 48 hours the RPE cells were significantly lost, leaving bare Bruch's membrane (Figure 8). This finding demonstrated that the bleaching procedure by using hydrogen peroxide could lead to artifact of RPE injury. Therefore, fluorescence microscopy of pigmented RPE cells without bleaching appears to be a better method.

4.4. Morphology of RPE cells varies with species

RPE cells vary in the morphology, size and the number of nuclei among species (Figure 9-10). Most RPE cells in mouse, rat and rabbit have a characteristic hexagonal morphology and 1 or 2 nuclei (Figure 9 A-D); but in the pig and monkey eyes, most RPE cells are round and compact, and have 1 nucleus (Figure 9 E and F). The size of the RPE cells varied in the different species (Figure 9). Interestingly, RPE cells with more than 2 nuclei are observed in the eyes of rat and rabbit, and up to 9 nuclei were detected in some rat RPE cells (Figure 10).

4.5. The study of RBCC in animal models

After intravenous injection of sodium iodate (SI), the rats were killed and the eyes were enucleated at

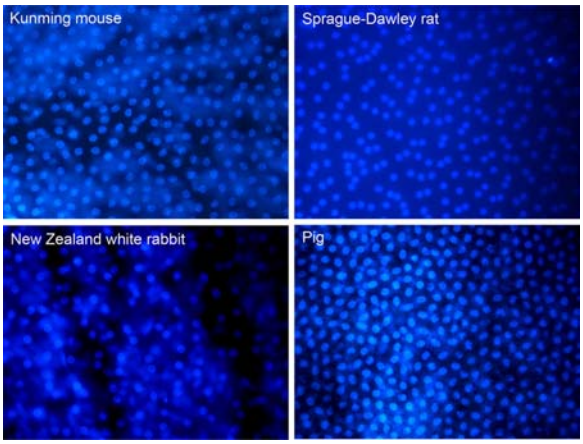

Figure 2. RBCC flatmount observation with DAPI staining. The RBCCs (from Kunming mouse, SD rat, New Zealand white rabbit and the domestic pig) were stained with DAPI (1 μg/mL) for 1 min, and examined under fluorescence microscope (400x).

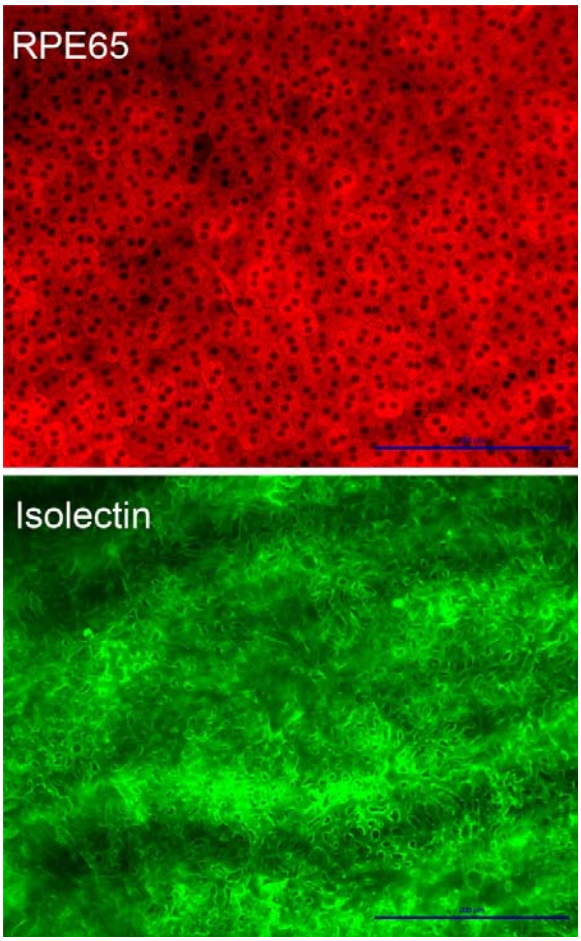

Figure 3. RPE monolayer and choriocapillaris examination in SD rats (200x). The RBCC was immunostained with 1) mouse anti-RPE65 (1:100, Santa Cruz, sc-53489) antibody and anti-mouse CY3 (1:100) secondary antibody for RPE cells examination (Red); and 2) Isolectin GS-IB4 (1:100, Invitrogen, 121411) for choriocapillaris endothelial cells examination (CCEs, green).

different time points for RPE evaluation by using RBCC methods. In normal rat, RPE cells were evenly distributed as a monolayer on RBCC (Figure 11). Compared with normal control, the RPE cells were significantly affected as early as 6 hours after intravenous injection of SI, and the damage was aggravated with increasing time (Figure 11). The changes included morphology alterations (swollen, enlarged cell gap); cell loss (single cell loss, patchy loss and massive cell loss with bare Bruch's membrane); RPE cell necrosis/apoptosis, abnormal cells with lipid-like structure and debris around, etc. From 6 to 12 hours after SI injection, RPE cells underwent initial injury period. RPE cells were easily detached from Bruch's membrane at this time to leave the Bruch's membrane bare. Figure 12 showed characteristic changes in RPE cells 2 weeks after SI injection. There were many "craters" surrounded with debris, indicating necrosis and massive loss of RPE cells (Figure 12A). Underneath these "craters", strong DAPI-positive stainings appeared, indicating the damage of RPE cells (Figure 12B).

We also studied RPE monolayer changes in RCS rats (Figure 13). In 2-week-old RCS rats, the dense microvilli and/or shed/ phagocytized discs of RPE cells blocked the direct view of RPE cell bodies. However, the nuclei are still evenly distributed with DAPI staining. In 100-day-old RCS rats, the RPE presented as disappeared microvilli, swollen and irregular cell bodies, and increased pigmentations; and the size and distribution of the nuclei presented a large variation. The time-dependent changes of RPE cells in RCS rats indicate the progressively damage of the RPE cells.

5. DISCUSSION

The retinal pigment epithelium (RPE) is a monolayer of multifunctional epithelial cells which physically abuts the photoreceptor layer and effectively forms the outer blood–retinal barrier (BRB). It plays a critical role in the maintenance of visual function. RPE cells contain photoprotective pigment granules, phagocytose shed photoreceptor outer segments (POS), recycle 11-cis retinal, and regulate ion and nutrient fluxes between the outer retina and choriocapillaris (1). And RPE cells also serve as the outer BRB that selectively transports biomolecules between the neurosensory retina and choriocapillaris, and releases various factors that protect the health and integrity of the outer retina, the choriocapillaris and the intervening Bruch's membrane (1). Degeneration or dysfunction of the RPE cells will lead to photoreceptor degeneration and visual impairment. For example, RPE cells lacking the Mer tyrosine kinase exhibit severely defective phagocytosis of POS and undergo rapid retinal degeneration (22, 23), and mutation or loss of RPE 65 in patients with Leber's Congenital Amaurosis leads to failure of the visual cycle and progressive retinal degeneration (7, 24). Because of the importance of the RPE cells and the limited methods for studying RPE cells, the present study is to establish a method for histological evaluation of RPE cells in RBCC flatmount.

The procedure for RBCC isolation is easy to perform, and this method is based on the anatomic

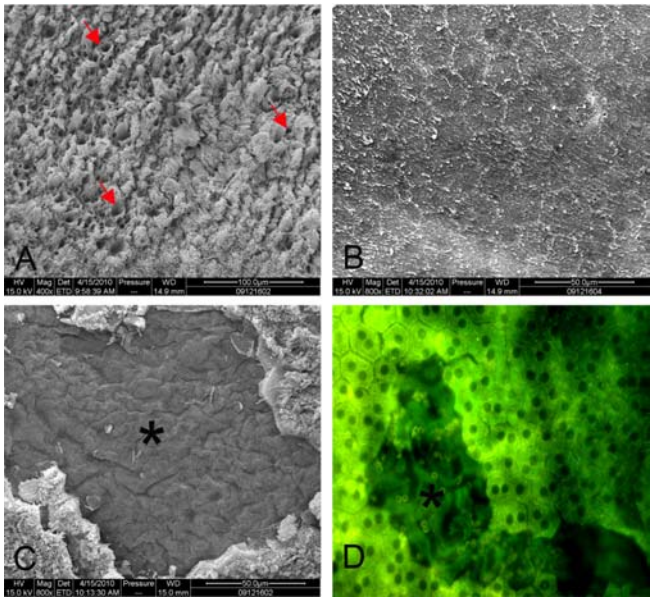

Figure 4. Rat RPE observed with SEM and fluorescence microscope. The microvilli (A, 400x), the morphology of RPE cells (B, 800x), and patchy RPE detachment (C, 800x) were observed under both SEM and fluorescence microscope (D, 400x). Multiple holes formed by the microvilli were indicated by red arrows (A), and the bare Bruch's membrane was indicated by black asterisk.

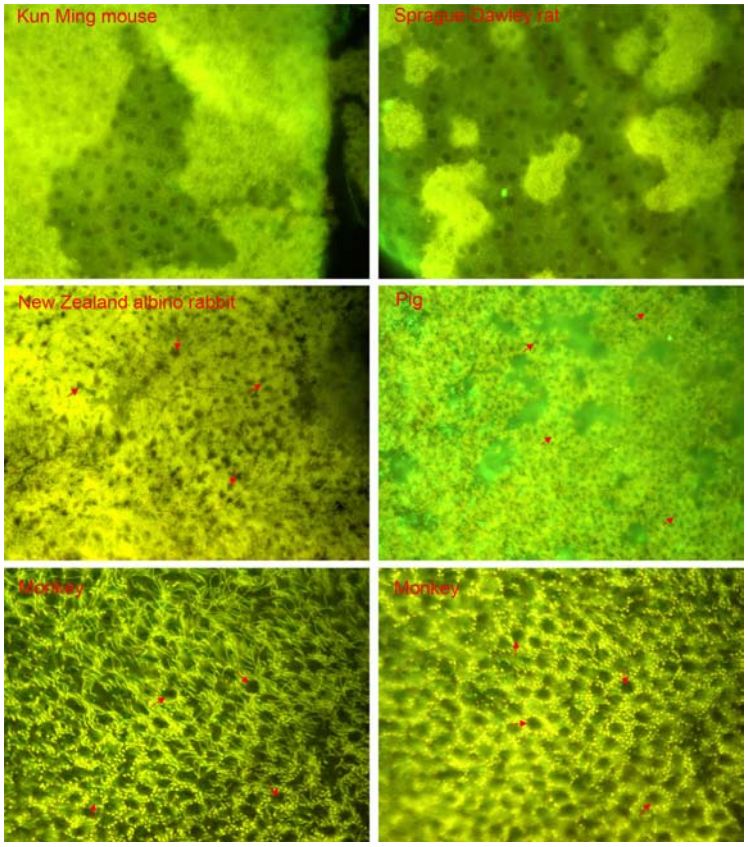

Figure 5. The appearance of RPE microvilli varying with species (400x). The microvilli of RPE cells are thinner in the eyes of mouse, rat and rabbit; and much larger in domestic pig and monkey. In rabbit, domestic pig and monkey eyes when the superior surface of the microvilli was focused, the microvilli of RPE cells present as the several holes (red arrow) where the outer segments of photoreceptors and the RPE cells are intertwining.

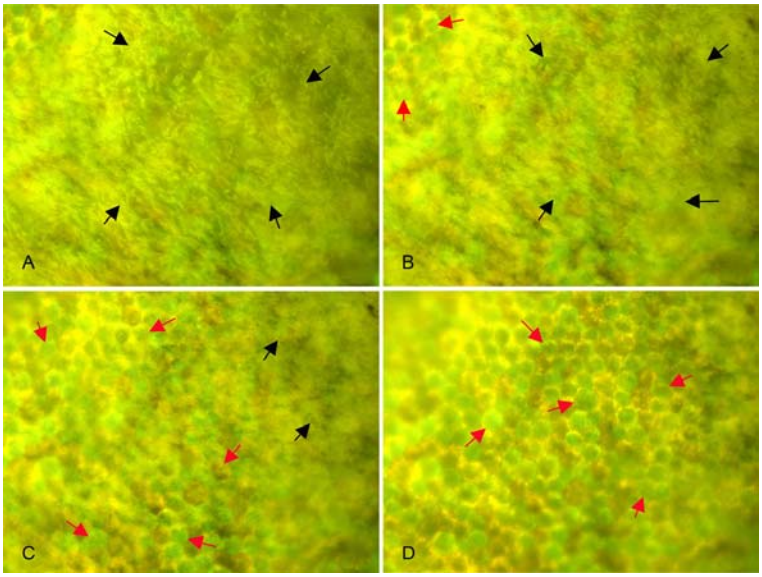

Figure 6. Monkey RPE microvilli observation. The microvilli were observed with fluorescence microscope (A→D, 400x) focusing from the top surface of the microvilli (A) to the deeper levels of RPE cells (B to D). The microvilli are indicated by black arrows; the RPE cell bodies were indicated by the red arrows.

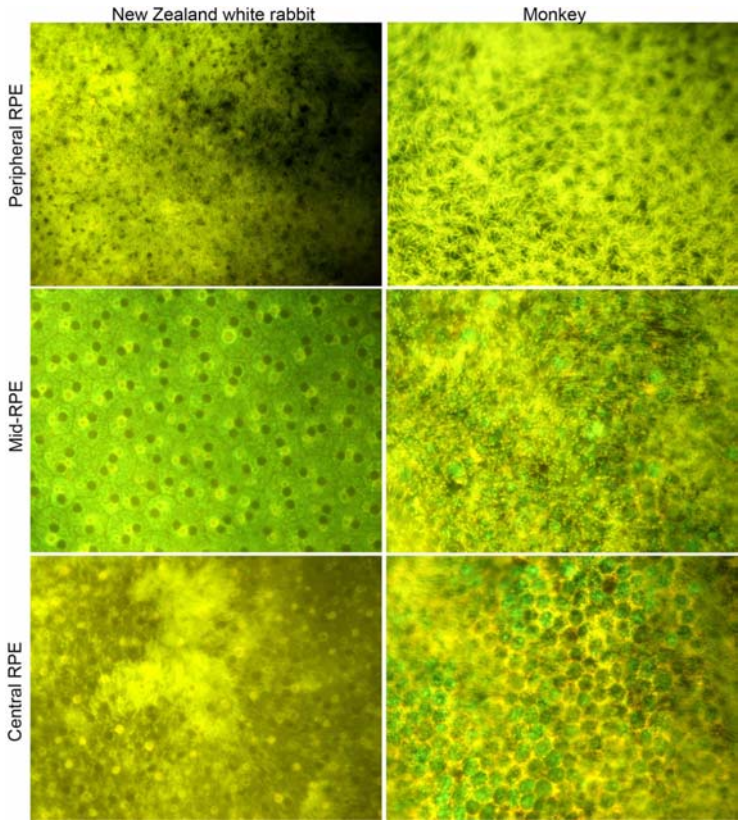

Figure 7. The distribution of microvilli. The microvilli were observed from the peripheral to the central RPE in the eyes of rabbit and monkey (400x). In rabbit, the microvilli are dense in peripheral RPE; less in central RPE, and nearly no microvilli detected in Mid-RPE; in monkey eye, the density of the microvilli gradually decreases from the peripheral to the central RPE, suggesting a trend showing more microvilli interacting with a single photoreceptor in periphery than in center. The focus is at the same level of the microvilli from the peripheral to central RPE.

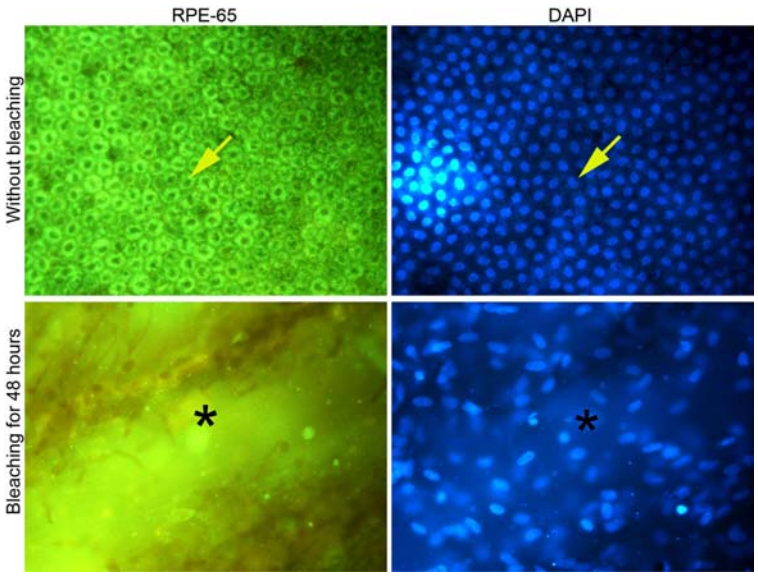

Figure 8. RPE flatmount of the domestic pig with or without bleaching (400x). The RBCC were immunostained with mouse anti-RPE65 antibody and anti-mouse (FITC) secondary antibody for RPE cells (Green); and DAPI staining for nuclei (Blue). The RPE cells are more compact with single nucleus (yellow arrow). After bleaching for 48 hours, the RPE cells were significantly lost leaving bare Bruch's membrane (black asterisk).

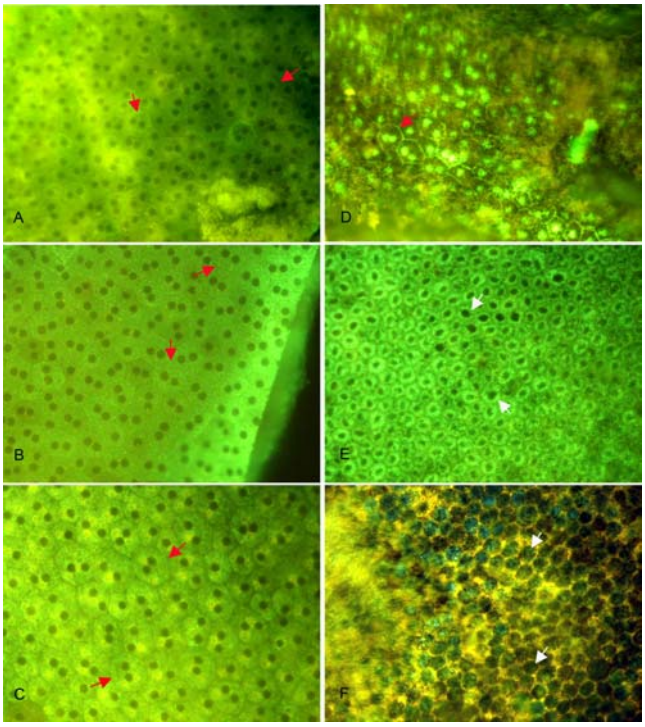

Figure 9. The variation of RPE cells in appearance from different species in both non-pigmented rodents (A-C) and pigmented animals (D-F). The RBCCs were immunostained with mouse anti-RPE65 antibody and anti-mouse (FITC) secondary antibody, and observed under fluorescence microscope (200x). (A) Kun Ming mouse, (B) Sprague-Dawley rat, (C) New Zealand white rabbit, (D) C57BL/6 mouse, (E) the domestic pig and (F) monkey. Most RPE cells in mouse (A and D), rat (B) and rabbit (C) have a characteristic hexagonal morphology and 1 or 2 nuclei (red arrow); but in the pig (E) and monkey (F) eyes, RPE cells are round and compact, and have 1 nucleus (white arrow). The size of RPE cells varied in different species.

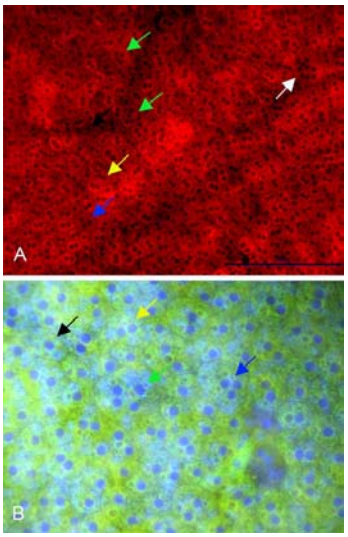

Figure 10. The observation of different numbers of nuclei in RPE cells from the same species. A: in rat (200x) and B: in rabbit (400x), e.g., 1 nucleus (black arrow); 2 nuclei (yellow arrow); 3 nuclei (blue arrow); 4 nuclei (green arrow), 6 nuclei (data not shown in rat) and 9 nuclei (white arrow).

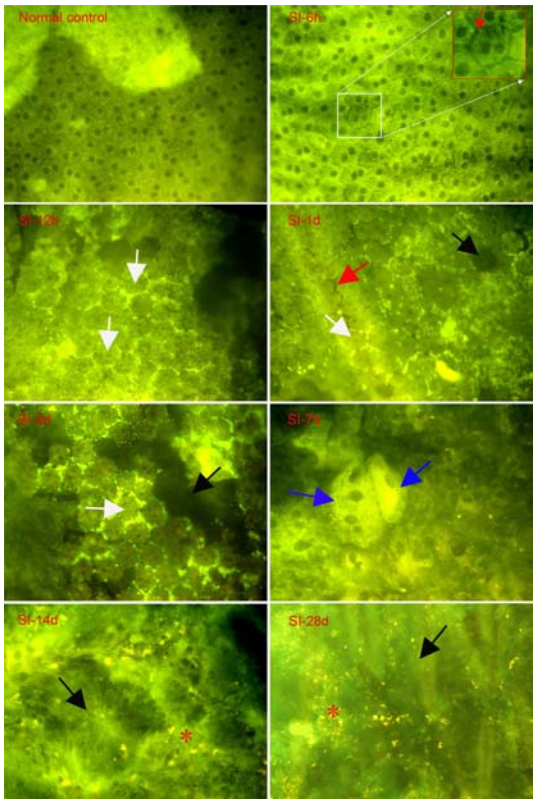

Figure 11. Rat RPE examinations after intravenous sodium iodate (SI, 50 mg/kg BW) injection (400x). RPE cells were significantly affected as early as 6 hours after SI injection (SI-6h), and the damage was aggravated with the progression of diseases. The changes include widened gap between RPE cells (SI-6h and SI-12h, red arrow); abnormal cells with lipid-like structure around (SI-12h, SI-1d and SI-3d, white arrow); RPE cell swollen or necrosis (SI-7d, blue arrow); RPE cell loss (black arrow): single cell dropout (SI-1d), patchy detachment (SI-3d) and massive cell loss (SI-14d and SI-28d) with debris leaving on the Bruch's membrane (red asterisk). SI-x h/d: time (hours or days) after sodium iodate injection.

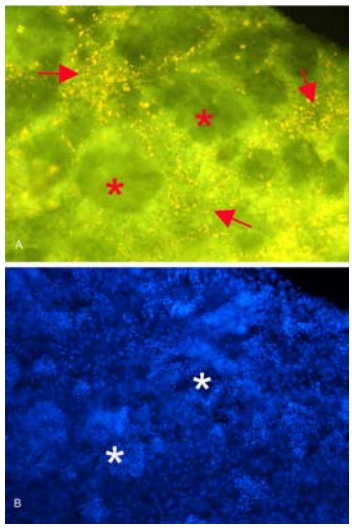

Figure 12. Rat RPE observations 2 weeks after intravenous sodium iodate injection (400x). After incubation in DAPI (1 μg/mL) for 1 min, the RBCC was first examined under fluorescence microscope in blue light channel (A), then the same field was switched to the UV channel (B). There are many "craters" (red asterisk) with surrounding debris (red arrow) on RBCC flatmount (A), indicating the necrosis and massive loss of RPE cells. Underneath these "craters", there appeared strong DAPI-positive stainings (white asterisk, B), indicating the damage of RPE cells.

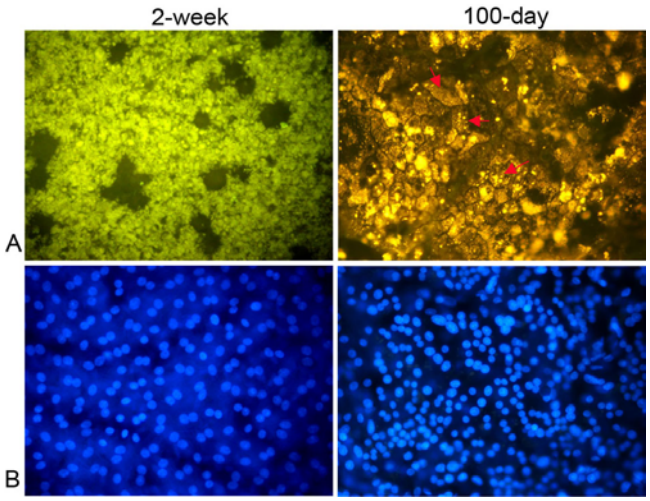

Figure 13. RPE observations of RCS rats with 2-week and 100-day age (400x). After incubation in DAPI (1 μg/mL) for 1 min, the RBCC was first examined under fluorescence microscope in blue light channel (A), and then the same field was switched to the UV channel (B). In 2-week-old RCS rats, the dense microvilli and/or shed/ phagocytized discs of RPE cells block the direct view of RPE cell bodies (A). However, the nuclei are still evenly distributed with DAPI staining (B). In 100-day-old RCS rats, the RPE (red arrow) presented as disappeared microvilli, swollen and irregular cell bodies, and increased pigmentations (A); and the size and distribution of the nuclei presented a large variation (B).

characteristics of the eye. There are two potential spaces, i.e., between the RBCC and neurosensory retina (subretinal space) and between the RBCC and sclera (suprachoroidal space). Compared with the process for cryosections, paraffin sections, and electron microscopy examination, this method is easy to perform and timesaving. After peeling off the neurosensory retina from the eye cup, the RBCC then was isolated from the sclera. The evaluation of the RBCC can be easily done by using fluorescence microscope and specific cellular markers conjugated with fluorescent dyes allowed visualization of different layers of the RBCC (RPE monolayer and choriocapillaris) (Figure 3). RPE 65 antibody and the appropriate secondary antibody conjugated to fluorochrome FITC or CY3 were used to label the RPE cells (Figure 3 and 9). Isolectin GS-IB4, a lectin derived from the seeds of *Griffonia simplicifolia*, has specific affinity for α-D-galactosyl residues and has been used for specifically labeling endothelial cells and microglia in a number of species. It was conjugated with the fluorochrome Alexa Fluor 488, to

outline the vessels, especially choriocapillaris endothelial cells, in green (Figure 3). DAPI, a nuclear stain with specific affinity for double-stranded DNA, was used to visualize the nuclei in blue (Figure 2).

Under the fluorescence microscope, the RBCC was well evaluated with the morphology and size of the cell bodies (Figure 9), the distribution and the number of the nuclei (Figure 2), the morphology and density of the apical villi (Figure 5-7), etc. For example, the distribution and density of the apical villi is varying among species, the density of the apical microvilli in monkey decreased from peripheral to central RPE (Figure 7), suggesting a trend showing more microvilli interacting with a single photoreceptor in periphery than in center. The nucleus numbers also vary among species; most RPE cells have 1 nucleus in primate and the domestic pig (Figure 8-9), but normally have 2 in mice, rat and rabbit (Figure 9). It is interesting that more than 2 nuclei were found in some of the RPE cells of the rat and rabbit (Figure 10). For instance, up to 9 nuclei were detected in rat RPE cells. The significance of a single RPE cell with multiple nuclei is not understood. For pigmented RPE cells, RPE can be directly observed without bleaching (Figure 8). The dropout of the RPE cells from the Bruch's membrane during bleaching process (Figure 8) was avoided in this method.

Two models of RPE degeneration were studied with this method in this study. In sodium iodate injected rat, the necrosis and dropout of the RPE cells with bare Bruch's membrane were clearly observed (Figure 11-12). The damage of RPE cells were gradually aggregated in RCS rats with disease progression and the cells become more compact with DAPI staining (Figure 13).

In conclusion, we developed a histoimmunochemistry-assisted method for evaluation of RPE cells within an intact RBCC. By using this method, we found that RPE cells are species specific varying in morphology; and the distribution of microvilli density from peripheral to central RPE cells is also varying among species. The pigmented RPE cells can be directly observed without bleaching, which favors its application in the further study with the eyes of the primate and human beings. This method has several advantages to study the changes of RPE cells, i.e., short time and less effort to manipulate the samples, *en bloc* examination to get a fair understanding of the whole RPE cell changes, and high efficiency for results readout. For a comprehensive evaluation of RPE changes in fundus diseases, e.g., AMD, diabetic retinopathy, retinitis pigmentosa, etc, this technique may be an adjunctive method to other methods such as cryosections/paraffin sections, electron microscopy, etc.

6. ACKNOWLEDGEMENT

Jingfa Zhang and Guoxu Xu are co-first authors. Drs Weiye Li and Guo-Tong Xu are co-corresponding authors, who contributed equally to this study. This work was supported by the following research grants: The National Basic Research Program (973 Program, No. 2007CB945004; No. 2009CB941100; and No. 2011CB965102); National Natural Science Foundation of China (No. 81000383); Research Fund for the Doctoral Program of Higher Education of China (No. 20100072120051); and Program of Tongji University (No. 1500219024; No. 2010QH04 and No. 2010YF02).

7. REFERENCES

1. O. Strauss: The retinal pigment epithelium in visual function. *Physiol Rev*, 85(3), 845-81 (2005)

2. R. Simo, M. Villarroel, L. Corraliza, C. Hernandez and M. Garcia-Ramirez: The retinal pigment epithelium: something more than a constituent of the blood-retinal barrier--implications for the pathogenesis of diabetic retinopathy. *J Biomed Biotechnol*, 2010, 190724

3. R. H. Steinberg: Interactions between the retinal pigment epithelium and the neural retina. *Doc Ophthalmol*, 60(4), 327-46 (1985)

4. G. M. Holtkamp, A. Kijlstra, R. Peek and A. F. de Vos: Retinal pigment epithelium-immune system interactions: cytokine production and cytokine-induced changes. *Prog Retin Eye Res*, 20(1), 29-48 (2001)

5. H. Morimura, G. A. Fishman, S. A. Grover, A. B. Fulton, E. L. Berson and T. P. Dryja: Mutations in the RPE65 gene in patients with autosomal recessive retinitis pigmentosa or leber congenital amaurosis. *Proc Natl Acad Sci U S A*, 95(6), 3088-93 (1998)

6. E. Margalit and S. R. Sadda: Retinal and optic nerve diseases. *Artif Organs*, 27(11), 963-74 (2003)

7. S. Hanein, I. Perrault, S. Gerber, G. Tanguy, F. Barbet, D. Ducroq, P. Calvas, H. Dollfus, C. Hamel, T. Lopponen, F. Munier, L. Santos, S. Shalev, D. Zafeiriou, J. L. Dufier, A. Munnich, J. M. Rozet and J. Kaplan: Leber congenital amaurosis: comprehensive survey of the genetic heterogeneity, refinement of the clinical definition, and genotype-phenotype correlations as a strategy for molecular diagnosis. *Hum Mutat*, 23(4), 306-17 (2004)

8. S. P. Daiger, S. J. Bowne and L. S. Sullivan: Perspective on genes and mutations causing retinitis pigmentosa. *Arch Ophthalmol*, 125(2), 151-8 (2007)

9. P. F. Lopez and T. M. Aaberg: Phenotypic similarities between Stargardt's flavimaculatus and pattern dystrophies. *Aust N Z J Ophthalmol*, 20(3), 163-71 (1992)

10. J. Z. Nowak: Age-related macular degeneration (AMD): pathogenesis and therapy. *Pharmacol Rep*, 58(3), 353-63 (2006)

11. R. D. Jager, W. F. Mieler and J. W. Miller: Age-related macular degeneration. *N Engl J Med*, 358(24), 2606-17 (2008)

12. K. C. Dunn, A. E. Aotaki-Keen, F. R. Putkey and L. M. Hjelmeland: ARPE-19, a human retinal pigment epithelial cell line with differentiated properties. *Exp Eye Res*, 62(2), 155-69 (1996)

13. A. Maminishkis, S. Chen, S. Jalickee, T. Banzon, G. Shi, F. E. Wang, T. Ehalt, J. A. Hammer and S. S. Miller: Confluent monolayers of cultured human fetal retinal pigment epithelium exhibit morphology and physiology of native tissue. *Invest Ophthalmol Vis Sci*, 47(8), 3612-24 (2006)

14. S. Sonoda, C. Spee, E. Barron, S. J. Ryan, R. Kannan and D. R. Hinton: A protocol for the culture and differentiation of highly polarized human retinal pigment epithelial cells. *Nat Protoc*, 4(5), 662-73 (2009)

15. K. Kiuchi, K. Yoshizawa, N. Shikata, K. Moriguchi and A. Tsubura: Morphologic characteristics of retinal degeneration induced by sodium iodate in mice. *Curr Eye Res*, 25(6), 373-9 (2002)

16. V. Enzmann, B. W. Row, Y. Yamauchi, L. Kheirandish, D. Gozal, H. J. Kaplan and M. A. McCall: Behavioral and anatomical abnormalities in a sodium iodate-induced model of retinal pigment epithelium degeneration. *Exp Eye Res*, 82(3), 441-8 (2006)

17. L. M. Franco, R. Zulliger, U. E. Wolf-Schnurrbusch, Y. Katagiri, H. J. Kaplan, S. Wolf and V. Enzmann: Decreased visual function after patchy loss of retinal pigment epithelium induced by low-dose sodium iodate. *Invest Ophthalmol Vis Sci*, 50(8), 4004-10 (2009)

18. E. F. Nandrot and E. M. Dufour: Mertk in daily retinal phagocytosis: a history in the making. *Advances in experimental medicine and biology*, 664, 133-40 (2010)

19. A. J. Carr, A. A. Vugler, S. T. Hikita, J. M. Lawrence, C. Gias, L. L. Chen, D. E. Buchholz, A. Ahmado, M. Semo, M. J. Smart, S. Hasan, L. da Cruz, L. V. Johnson, D. O. Clegg and P. J. Coffey: Protective effects of human iPS-derived retinal pigment epithelium cell transplantation in the retinal dystrophic rat. *PLoS One*, 4(12), e8152 (2009)

20. A. Oganesian, E. Bueno, Q. Yan, C. Spee, J. Black, N. A. Rao and P. F. Lopez: Scanning and transmission electron microscopic findings during RPE wound healing *in vivo*. *Int Ophthalmol*, 21(3), 165-75 (1997)

21. C. R. Braekevelt: Fine structure of the retinal epithelium (RPE) of the emu (Dromaius novaehollandiae). *Tissue Cell*, 30(2), 149-56 (1998)

22. P. M. D'Cruz, D. Yasumura, J. Weir, M. T. Matthes, H. Abderrahim, M. M. LaVail and D. Vollrath: Mutation of the receptor tyrosine kinase gene Mertk in the retinal dystrophic RCS rat. *Hum Mol Genet*, 9(4), 645-51 (2000)

23. A. Gal, Y. Li, D. A. Thompson, J. Weir, U. Orth, S. G. Jacobson, E. Apfelstedt-Sylla and D. Vollrath: Mutations in MERTK, the human orthologue of the RCS rat retinal dystrophy gene, cause retinitis pigmentosa. *Nat Genet*, 26(3), 270-1 (2000)

24. S. M. Gu, D. A. Thompson, C. R. Srikumari, B. Lorenz, U. Finckh, A. Nicoletti, K. R. Murthy, M. Rathmann, G. Kumaramanickavel, M. J. Denton and A. Gal: Mutations in RPE65 cause autosomal recessive childhood-onset severe retinal dystrophy. *Nat Genet*, 17(2), 194-7 (1997)

Abbreviations: AMD: age-related macular degeneration; BRB: blood-retinal barrier; CCE: Choriocapillaris endothelial cells; POS: photoreceptor outer segments; RBCC: RPE-Bruch's membrane-choriocapillaris complex; RPE: retinal pigment epithelium; SEM: scanning electronic microscope

Key Words: Choriocapillaris; CCE; Retinal pigment epithelium; RPE; RPE-Bruch's membrane-choriocapillaris complex; RBCC

Send correspondence to: Guo-Tong Xu, Tongji Eye Institute and Department of Regenerative Medicine, Tongji University School of Medicine, 1239 Siping Road, Medical School Building, Room 521, Shanghai, 200092, China, Tel: 86-21-6598-6358, Fax: 86-21-6598-6358, E-mail: gtxu@tongji.edu.cn

http://www.bioscience.org/current/vol4E.htm